

# Toward uniform nanotubular compounds: Synthetic approach and *ab initio* calculations

Glen P. Miller<sup>a)</sup>

Department of Chemistry, University of New Hampshire, Durham, New Hampshire 03824

Shinya Okano and David Tománek

Physics and Astronomy Department, Michigan State University, East Lansing, Michigan 48824

(Received 23 January 2006; accepted 23 February 2006; published online 31 March 2006)

We propose to synthesize a new class of single-walled nanotubular compounds (SWNCs) and investigate the interplay between their structural and electronic properties using *ab initio* density functional calculations. SWNCs are composed of cyclacenes of variable diameter interconnected by various linker compounds. Cyclacenes map directly onto and can be viewed as the shortest segments of  $(n,0)$  zigzag carbon nanotubes. We focus on cyclacenes with  $n=6-12$  fused benzene rings interconnected by biphenyl, tetrazine, or acetylene linkers. Depending upon the nature and the orientation of the linkers, we find it possible to change the systems from narrow-gap to wide-gap semiconductors, and to modulate the band dispersion, suggesting the possibility of band gap engineering. © 2006 American Institute of Physics. [DOI: 10.1063/1.2187968]

Combining atomic-scale perfection with length extending to millimeters, carbon nanotubes<sup>1</sup> are unique polymers with applications ranging from structural reinforcement of composites to molecular wires for a new generation of electronic devices.<sup>2,3</sup> Because all current synthetic processes involve high temperatures, the raw product invariably contains a distribution of nanotube diameters and chiral angles, often with catalyst impurities. Since the conductivity of nanotubes depends sensitively on their diameter and chiral winding angle,<sup>4-6</sup> application of nanotubes in molecular electronics devices requires nanotubes with a well-defined structure. Whereas several approaches have been developed to separate SWNTs (post-synthesis) into metallic and semiconducting species,<sup>7-10</sup> a bottom-up synthesis of uniform SWNTs with variable diameter and chiral winding angle has yet to be achieved.

Here, we propose to synthesize a new class of single-walled nanotubular compounds (SWNCs), related to carbon nanotubes, and study their physical properties. The synthetic pathway is a low temperature, selective, wet chemical approach designed to yield uniform batches of SWNCs. This synthesis has its origins in [60]fullerene chemistry, and includes the conversion of acenes into cyclacenes, followed by the iterative oligomerization/transformation of cyclacenes into SWNCs.

The proposed synthetic approach is inspired by our results of the Diels-Alder chemistry between [60]fullerenes and large acenes.<sup>11</sup> With proper phenyl substitution along the acene backbone, we identified conditions to cycloadd two<sup>12</sup> and three<sup>13</sup> [60]fullerenes across a single acene. Remarkably, the [60]fullerenes are found to add across phenyl substituted acenes in a diastereoselective *syn* fashion. Further studies have revealed that [60]fullerene-[60]fullerene  $\pi$ - $\pi$  stacking

interactions are responsible for the highly selective *syn* additions.<sup>14</sup>

More than a scientific curiosity, the *syn* addition of multiple [60]fullerenes across large acenes suggests the possibility of using this chemistry to literally roll-up acenes to form cyclacene structures. Figure 1(a) illustrates a proposed pathway for which synthetic work is ongoing. In Fig. 1(b), an iterative oligomerization of cyclacenes to SWNCs is illustrated. In this manner, we propose to build a library of SWNCs, each batch composed of uniform molecules with precisely controlled length and diameter.

Complementing the synthesis efforts, we have performed *ab initio* calculations addressing the equilibrium geometry, stability, and electronic structure of SWNCs including the

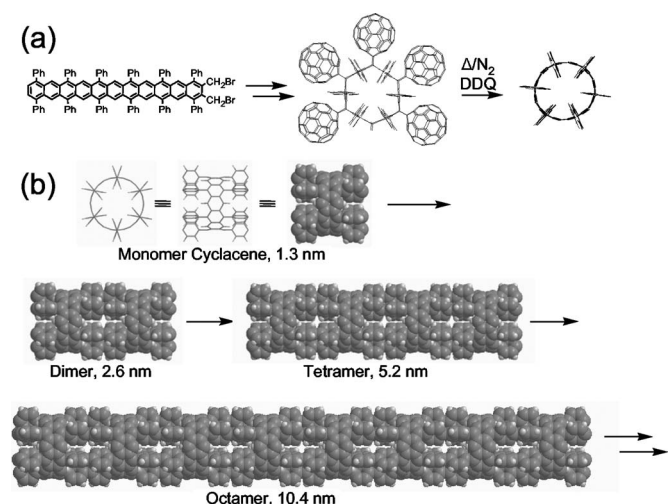


FIG. 1. Proposed synthesis of SWNCs using cyclacenes. (a) Diastereoselective *syn* addition of [60]fullerenes across a phenyl substituted undecacene followed by cyclization and retro-Diels-Alder removal of [60]fullerenes. (b) Iterative oligomerization of phenyl substituted cyclacenes to form SWNCs with precisely controlled lengths and diameters.

<sup>a)</sup> Author to whom correspondence should be addressed. Electronic mail: glen.miller@unh.edu

fundamental band gap, charge distribution, and character of wave functions. We consider SWNCs composed of cyclacenes with  $n=6-12$  fused benzene rings, as well as infinitely large cyclacenes corresponding to narrow graphene ribbons. The cyclacenes are interconnected by biphenyl, tetrazine, or acetylene linkers, and the results are compared to 2D periodic systems of interconnected acene ribbons. Depending upon the nature and the orientation of the linkers, we find it possible to change the systems from narrow-gap to wide-gap semiconductors, and to modulate the band dispersion, suggesting the possibility of band gap engineering.

Our *ab initio* density-functional theory (DFT) calculations<sup>15</sup> of SWNCs are performed within the local-density approximation (LDA).<sup>16</sup> We use a double-zeta localized orbital basis with polarization functions, Troullier-Martins *ab initio* pseudopotentials to describe the interaction of valence electrons with atomic nuclei and core electrons,<sup>17</sup> and the Perdew-Zunger<sup>18</sup> form of the exchange-correlation potential,<sup>19</sup> as implemented in the SIESTA code.<sup>20,21</sup> The range of the localized orbitals is limited in such a way that the energy shift<sup>22,23</sup> caused by their spatial confinement is only 100 meV. The charge density and potentials are calculated on a real-space grid with a mesh cutoff energy of 150 Ry, which is sufficient to achieve a total energy convergence of 1 meV/atom during the self-consistency iterations. Periodic boundary conditions are used in all directions, keeping a minimum interatomic separation of 7 Å to suppress unwanted interactions between periodic replicas. The Brillouin zone of the one-dimensional polymers is sampled by 2 or 4  $k$ -points, and that of two-dimensional linked acene layers by a  $6 \times 8$   $k$ -point grid.<sup>24</sup> Full optimization of the systems of interest is performed to determine the optimum geometry, the total energy, and the electronic structure. A structure is considered to be optimized when none of the residual forces acting on atoms exceeds the value 0.04 eV/Å.

The equilibrium geometry and electronic states of a SWNC composed of 12-membered cyclacene rings interconnected by biphenyl linkers is shown in Fig. 2. Global optimization of this system was computationally challenging due to the large number of atoms (180) per unit cell. A set of optimizations was performed for lattice constants ranging from 12.8 to 13.2 Å, containing one cyclacene ring and the linkers. As an initial guess, all linkers were rotated by the same angle in the same direction. For each value of the lattice constant, the structure was then globally optimized using the conjugate gradient technique. The unit cell size in the optimum SWNC structure was found to be 13.01 Å. The side view of the SWNC in Fig. 2(a) and the end-on view in Fig. 2(b) show how adjacent cyclacenes are interconnected by six biphenyl linkers. Since 12-membered cyclacene rings are the shortest segments of a (12,0) zigzag carbon nanotube, the carbon nanotube nomenclature is extended to include cyclacene-based SWNCs. In the most stable structure, the biphenyl linkers are rotated by  $\theta \approx 70^\circ$  with respect to the tube surface. In view of the optimum linker arrangement depicted in Fig. 2(b), the minimum nanotube diameter is expected to be limited by the spatial requirements of the linkers. This fact is of importance when pursuing a wet chemical synthesis of  $(n,0)$  zigzag SWNCs.

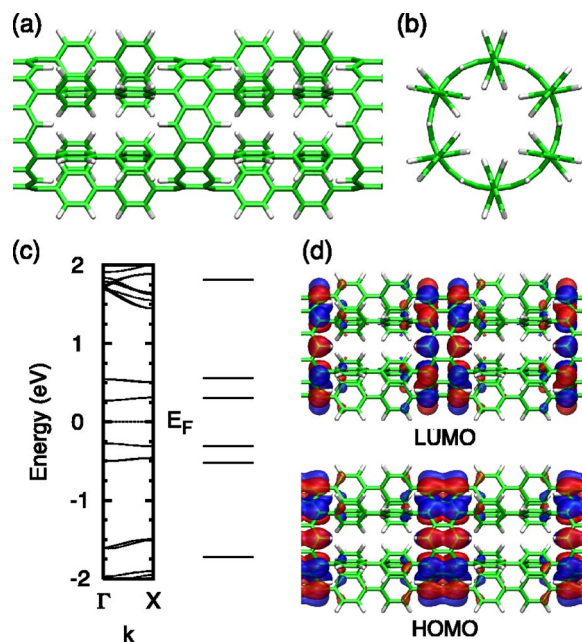


FIG. 2. (Color online) (12,0) cyclacene-based SWNC with biphenyl linkers. (a) Side view and (b) end-on view of a stick model depicting two unit cells of the SWNC. (c) Band structure of the infinite polymer, compared to electronic levels of a 12-membered cyclacene molecule on the right. The Fermi level is set as  $E_F=0$ . (d) Isosurfaces of the HOMO and LUMO states at the  $\Gamma$  point for the (12,0) tube, presented at  $\rho=0.03$  e/Å<sup>3</sup>. The phase of the orbitals is distinguished by color.

The large binding energy of the cyclacene-based  $C_{120}H_{60}$  SWNC,  $E_{\text{coh}}=1264.8$  eV per unit cell with respect to isolated atoms, reflects the calculated high stability of the  $C_{48}H_{24}$  cyclacene,  $E_{\text{coh}}=502.2$  eV, and of the  $C_{12}H_{10}$  biphenyl linker,  $E_{\text{coh}}=140.8$  eV. Since most atoms in the SWNC can be associated with the cyclacene rings, which are closely related to a zigzag carbon nanotube of the same diameter, the polymeric SWNC should be almost as stable as a conventional SWNT. Indeed, the average binding energy per atom in the polymeric SWNC,  $E_{\text{coh}}(C_{120}H_{60})/180=7.0$  eV, compares favorably even with the binding energy per atom in graphite,  $E_{\text{coh}}=7.3$  eV.

The band structure of the (12,0) cyclacene-based SWNC is shown Fig. 2(c). The six bands (two of them doubly degenerate) closest to the Fermi level show very little dispersion of less than 0.04 eV and are closely related to the corresponding energy levels of an individual cyclacene molecule, shown on the right of the band structure. The fundamental gap of the cyclacene-based SWNC of 0.55 eV lies very close to the calculated HOMO-LUMO gap of the cyclacene molecule, suggesting semiconducting behavior of the polymeric SWNC. Here, we should emphasize that the finite HOMO-LUMO gap in the individual cyclacene molecule, viewed as a (12,0) nanotube segment, arises due to its short length; the band gap vanishes in the infinite (12,0) carbon nanotube.<sup>4-6</sup> Since LDA calculations typically underestimate the fundamental gap, the observed optical gap should be much larger than the LDA gap.

The electronic states near the Fermi level of the polymeric SWNC and an isolated cyclacene molecule are similar not only in their energy spacing, but also in their character.

The HOMO-1 and LUMO+1 levels of the cyclacene are doubly degenerate, similar to the second valence band from the top and the second conduction band from the bottom in the infinite system. Additionally, the charge distribution in the highest occupied and lowest unoccupied states of the cyclacene is similar to that in the corresponding band states of the polymeric SWNC, depicted at the  $\Gamma$  point in Fig. 2(d). The corresponding wave functions are almost completely localized on the cyclacene rings, with no amplitude on the linkers. This complements the finding that linker states are separated from the Fermi level by at least 2 eV, not providing any indirect coupling between the frontier orbitals on adjacent cyclacene rings.

The absence of coupling between the cyclacenes and the linkers can be understood from the way the linkers are attached to the cyclacene rings. The large dihedral angle of nearly  $70^\circ$  all but destroys  $\pi$  conjugation between the rings and linkers and thus is responsible for opening a gap and isolating the frontier orbitals of adjacent cyclacenes in space. This effective decoupling of the wave functions associated with adjacent cyclacenes ultimately causes the small band dispersion seen in Fig. 2(c). In terms of electronic response, this cyclacene-based SWNC should behave like a chain of nearly decoupled quantum dots with quantum transport dominated by Coulomb blockade behavior.

Besides the (12,0) SWNCs, the equilibrium geometry and electronic states in the (8,0) and (6,0) cyclacene-based SWNCs were also investigated. In these narrower tubes, there is strain associated with rolling up isolated acenes to cyclacenes, reducing their binding energy to  $E_{\text{coh}}(\text{C}_{32}\text{H}_{16}) = 331.4$  eV for the 8-membered cyclacene and to  $E_{\text{coh}}(\text{C}_{24}\text{H}_{12}) = 244.7$  eV in the 6-membered cyclacene. As the SWNCs become narrower, the biphenyl linkers become spatially closer inside the tube and hinder each others rotation. This hindrance results in additional strain energy since the linkers are no longer free to independently find their optimum conformations. Both sets of strain energies contribute to the total energetic cost associated with rolling up layers of planar acene strips to form  $(n,0)$  cyclacene-based SWNCs. Per unit cell of the  $(n,0)$  SWNC, the strain energy is defined as  $E_{\text{roll}}(n,0) = (E_{\text{tube}} - E_{\text{sheet}})/n$ , and its value increases with decreasing tube diameter from  $E_{\text{roll}}(12,0) = 0.28$  eV to  $E_{\text{roll}}(8,0) = 0.77$  eV to  $E_{\text{roll}}(6,0) = 1.62$  eV. The similarity between the frontier orbitals of isolated cyclacenes and the corresponding SWNCs persists even in the narrower nanotubes.

In cyclacene-based SWNCs with biphenyl linkers, the effective decoupling of neighboring cyclacenes results from reduced  $\pi$  conjugation due to rotation of the linkers normal to the tube surface. A model calculation for infinitely long acene strips connected by biphenyl linkers shows that increasing the interlinker separation did not affect their preferred orientation with respect to the acene plane. The optimum degree of rotation appears to be intrinsic to the biphenyl-acene bond. To enhance the degree of  $\pi$  conjugation in the axial direction, other linkers with a smaller preferential dihedral angle  $\theta$ , corresponding to a smaller rotation away from the tube surface, were considered. Assuming that the large optimum value  $\theta \approx 70^\circ$  in the case of biphenyl linkers is caused by repulsion between *ortho* hydrogen atoms on

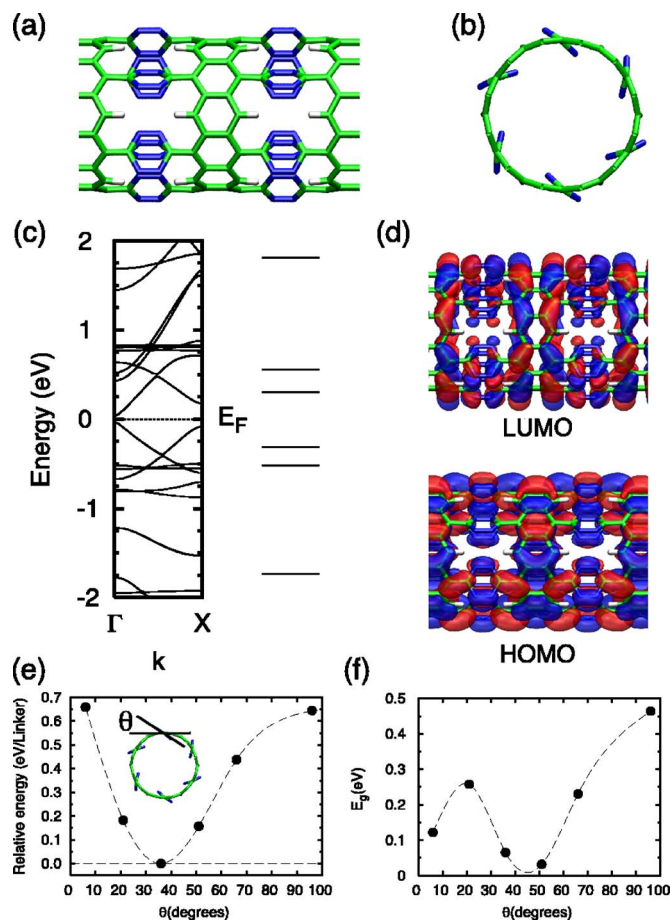


FIG. 3. (Color online) (12,0) Cyclacene-based SWNC with tetrazine linkers. (a) Side view and (b) end-on view of a stick model depicting two unit cells of the SWNC. (c) Band structure of the infinite polymeric SWNC compared to electronic levels of a 12-membered cyclacene molecule on the right. The Fermi level is set as  $E_F=0$ . (d) Isosurfaces of the HOMO and LUMO states at the  $\Gamma$  point for the (12,0) tube, presented at  $\rho=0.03$  e/ $\text{\AA}^3$ . The phase of the orbitals is distinguished by color. (e) Energy of the (12,0) SWNC as a function of the tetrazine linker angle  $\theta$ , relative to the reference value for the equilibrium structure with  $\theta \approx 36^\circ$ . (f) HOMO-LUMO gap energy  $E_g$  of the system as a function of  $\theta$ . The dashed lines in (e) and (f) are guides for the eye.

the biphenyl rings and the cyclacenes, an alternative choice is to use a linker like 1,2,4,5-tetrazine, which possesses no *ortho* hydrogen atoms.

The equilibrium geometry and electronic states for a SWNC based on 12-membered cyclacene rings interconnected by 1,2,4,5-tetrazine linkers are shown in Fig. 3. The large binding energy of the tetrazine-based  $\text{C}_{60}\text{H}_{12}\text{N}_{24}$  SWNC,  $E_{\text{coh}} = 765.6$  eV per unit cell with respect to isolated atoms, derives mainly from the high stability of the cyclacene, and to a smaller degree the six  $\text{C}_2\text{H}_2\text{N}_4$  tetrazine molecules per unit cell, with  $E_{\text{coh}} = 44.7$  eV. With 96 atoms per unit cell, global optimization was less challenging than in SWNCs containing biphenyl linkers. An analogous optimization procedure yielded 8.44  $\text{\AA}$  as the equilibrium lattice constant. The side view of the polymer in Fig. 3(a) and the end-on view in Fig. 3(b) show how adjacent cyclacenes are interconnected by six tetrazine linkers. As suggested earlier, in the absence of *ortho* hydrogen-hydrogen repulsion, the tetrazine linkers are expected to be closer to the desired coplanar geometry with improved  $\pi$  conjugation. The optimum



value of the dihedral angle between the linkers and the tube surface is found to be  $\theta \approx 36^\circ$ , shown in Fig. 3(b), confirming this expectation. With improved  $\pi$  conjugation along the tube axis, the electronic systems of the cyclacenes are no longer decoupled. As a consequence, the band structure of the (12,0) cyclacene-based SWNC with tetrazine linkers, shown in Fig. 3(c), bears very little resemblance to the electronic structure of the cyclacene molecules, shown on the right. In fact, the band dispersion, caused by increased hybridization, nearly fills the entire HOMO-LUMO gap of cyclacene, reducing the fundamental gap of the polymeric SWNC to  $E_g = 0.07$  eV at the  $\Gamma$  point. As shown in Fig. 3(d), the charge distribution at the top of the valence band and the bottom of the conduction band results in a strong delocalization of the highest occupied and lowest unoccupied states. In stark contrast to cyclacenes interconnected by biphenyl linkers, the frontier orbitals extend across both the cyclacenes and the tetrazine linkers in the optimum geometry. In terms of transport behavior, an I-V characteristic reminiscent of conventional bulk semiconductors, with no Coulomb-blockade steps, is expected.

In view of the large difference in band dispersions between SWNCs prepared with biphenyl and tetrazine linkers, modifying the characteristic twist angle  $\theta$  between linker and cyclacene is tantamount to band gap engineering. Thus, the wet chemical synthesis of SWNCs potentially offers a wide range of uniform, tunable molecular nanowires, each custom designed for a unique application.

To investigate the energy effort associated with linker rotation, the energy of the resulting SWNC was studied as a function of the dihedral angle  $\theta$  between the tetrazine and the tube surface. Using the optimum geometry of  $\theta = 36^\circ$  as a reference, all linkers were rigidly rotated in the same direction by  $-30^\circ$ ,  $-15^\circ$ ,  $15^\circ$ ,  $30^\circ$ , and  $60^\circ$ . Since the rest of the structure was kept frozen, the results, shown in Fig. 3(e), are strictly upper bounds on the energy differences. Considering the high energy cost of nearly 0.5 eV required to twist the tetrazine from its optimum conformation to a coplanar or normal conformation, all linker angles should remain close to their optimum value in the absence of a serious perturbation. Figure 3(f) shows the dependence of the fundamental gap  $E_g$  on  $\theta$ . As mentioned earlier, a direct gap with  $E_g = 0.07$  eV is found at the  $\Gamma$  point in the optimum conformation with  $\theta = 36^\circ$ . Increasing the linker angle  $\theta$  reduces  $\pi$  conjugation along the wire direction, thus increasing the value of  $E_g$ .

In order to eliminate the effect of the twisting angle  $\theta$  from our discussion of axial  $\pi$  conjugation, acetylene was investigated as an alternative cyclacene linker. Instead of a finite-diameter tube, a periodic array of connected acene strips was investigated. The electronic structure of a (12,0) cyclacene-based SWNC with acetylene linkers was found by folding the 2D electronic bands into the 1D Brillouin zone of the tube. With only ten carbon and two hydrogen atoms per unit cell, the system was found to be quite stable with  $E_{\text{coh}}(\text{C}_{10}\text{H}_2) = 93.9$  eV compared to the binding energy of acetylene  $E_{\text{coh}}(\text{C}_2\text{H}_2) = 21.44$  eV. There are no rotational degrees of freedom associated with the acetylene linkers, which should favorably affect axial  $\pi$  conjugation. As expected, the

band dispersion in this system is large, but the fundamental gap  $E_g = 0.58$  eV remained as high as in isolated cyclacene molecules.

In conclusion, we have used *ab initio* density functional calculations to determine the equilibrium atomic structure, stability, and electronic states of SWNCs composed of cyclacenes interconnected by biphenyl, tetrazine, and acetylene linkers. Our results indicate that SWNCs prepared from 12-membered cyclacenes with biphenyl linkers are particularly stable. However, the large twist angle between the linker and the cyclacene surface significantly reduces axial  $\pi$  conjugation, effectively decoupling the electronic systems of the cyclacenes. Consequently, the electronic structure of SWNCs with biphenyl linkers, including the fundamental band gap, is found to lie close to that of isolated cyclacene molecules. Our calculations further predict that tetrazine linkers are superior to biphenyls in terms of maximizing the axial  $\pi$  conjugation, reducing the fundamental band gap, and allowing the electrons in frontier orbitals to delocalize across the entire system. The judicious choice of cyclacene linkers enables a controlled modification of the characteristic twist angle  $\theta$  between linker and cyclacene and is equivalent to band gap engineering. Most importantly, calculations of this type enable a more efficient synthesis of technologically relevant SWNCs with desired properties.

We gratefully acknowledge financial support by NSF NER Grant No. ECS-0403954 (G.P.M.), NSF NIRT Grant No. ECS-0506309 (D.T.), and the NSF NSEC Grant No. EEC-0425826 (G.P.M. and D.T.).

<sup>1</sup> *Carbon Nanotubes: Synthesis, Structure, Properties and Applications*, Topics in Applied Physics Vol. 80, edited by M. S. Dresselhaus, G. Dresselhaus, and P. Avouris (Springer-Verlag, Berlin, 2001).

<sup>2</sup> S. Heinze, J. Tersoff, R. Martel, V. Derycke, J. Appenzeller, and Ph. Avouris, *Phys. Rev. Lett.* **89**, 106801 (2002).

<sup>3</sup> F. Nihey, H. Hongo, M. Yudasaka, and S. Iijima, *Jpn. J. Appl. Phys.* **41**, L1049 (2002).

<sup>4</sup> J. W. Mintmire, B. I. Dunlap, and C. T. White, *Phys. Rev. Lett.* **68**, 631 (1992).

<sup>5</sup> N. Hamada, S. Sawada, and A. Oshiyama, *Phys. Rev. Lett.* **68**, 1579 (1992).

<sup>6</sup> R. Saito, M. Fujita, G. Dresselhaus, and M. S. Dresselhaus, *Appl. Phys. Lett.* **60**, 2204 (1992).

<sup>7</sup> M. S. Strano, C. A. Dyke, M. L. Usrey, P. W. Barone, M. J. Allen, H. W. Shan, C. Kittrell, R. H. Hauge, J. M. Tour, and R. E. Smalley, *Science* **301**, 1519 (2003).

<sup>8</sup> Z. Chen, X. Du, M-H. Du, C. D. Rancken, H-P. Cheng, and A. G. Rinzier, *Nano Lett.* **3**, 1245 (2003).

<sup>9</sup> D. Chattopadhyay, L. Galeska, and F. Papadimitrakopoulos, *J. Am. Chem. Soc.* **125**, 3370 (2003).

<sup>10</sup> M. Zheng, A. Jagota, E. D. Semke, B. A. Diner, R. S. McLean, S. R. Lustig, R. E. Richardson, and N. G. Tassi, *Nat. Mater.* **2**, 338 (2003).

<sup>11</sup> J. Mack and G. P. Miller, *Fullerene Sci. Technol.* **5**, 607 (1997).

<sup>12</sup> G. P. Miller and J. Mack, *Org. Lett.* **2**, 3979 (2000); G. P. Miller and J. Briggs, *Proceedings of the International Symposium on Fullerenes, Nanotubes, and Carbon Nanostructures*, Fullerenes Vol. 11, edited by P. V. Kamat, D. M. Guldi, and K. M. Kadish, 202 (The Electrochemical Society, Pennington, NJ, 2001); G. P. Miller, J. Briggs, J. Mack, P. A. Lord, M. M. Olmstead, and A. L. Balch, *Org. Lett.* **5**, 4199 (2003).

<sup>13</sup> G. P. Miller and J. Briggs, *Org. Lett.* **5**, 4203 (2003).

<sup>14</sup> G. P. Miller, J. Mack, and J. Briggs, *Org. Lett.* **2**, 3983 (2000); G. P. Miller and J. Briggs, *Tetrahedron Lett.* **45**, 477 (2004).

<sup>15</sup> P. Hohenberg and W. Kohn, *Phys. Rev. B* **136**, B864 (1964).

<sup>16</sup> W. Kohn and L. J. Sham, *Phys. Rev. A* **140**, A1133 (1965).

<sup>17</sup> N. Troullier and J. L. Martins, *Phys. Rev. B* **43**, 1993 (1991).

<sup>18</sup> J. P. Perdew and A. Zunger, *Phys. Rev. B* **23**, 5048 (1981).

<sup>19</sup>D. M. Ceperley and B. J. Alder, Phys. Rev. Lett. **45**, 566 (1980).

<sup>20</sup>P. Ordejón, E. Artacho, and J. M. Soler, Phys. Rev. B **53**, R10441 (1996).

<sup>21</sup>J. M. Soler, E. Artacho, J. D. Gale, A. García, J. Juquera, P. Ordejón, and D. Sánchez-Portal, J. Phys.: Condens. Matter **14**, 2745 (2002).

<sup>22</sup>O. F. Sankey and D. J. Niklewski, Phys. Rev. B **40**, 3979 (1989).

<sup>23</sup>E. Artacho, D. Sánchez-Portal, P. Ordejón, A. García, and J. M. Soler, Phys. Status Solidi B **215**, 809 (1999).

<sup>24</sup>H. J. Monkhorst and J. D. Pack, Phys. Rev. B **13**, 5188 (1976).